Solid-state chiral optical properties of axially chiral binaphthyl acid derivatives

Takafumi Kinuta[a], Tomohiro Sato[a], Yoko Nakano[b], Takunori Harada[c], Nobuo Tajima[d], Michiya Fujiki[b], Reiko Kuroda[c], Yoshio Matsubara[a,∗], Yoshitane Imai[a,∗]

[a] Department of Applied Chemistry, Faculty of Science and Engineering, Kinki University, 3-4-1 Kowakae, Higashi-Osaka, Osaka 577-8502, Japan
[b] Graduate School of Materials Science Nara Institute of School and Technology Takayama, Ikoma, Nara 630-0192, Japan
[c] Department of Life Sciences, Graduate School of Arts and Sciences, The University of Tokyo, 3-8-1 Komaba, Meguro-ku, Tokyo 153-8902, Japan
[d] Graduate School of Pure and Applied Sciences, Tsukuba University, 1-1-1 Tenodai, Tsukuba, Ibaraki 305-8571, Japan

ARTICLE INFO

ABSTRACT

It is important to first determine the solid-state chiral optical properties of basic fluorescence supramolecular building blocks that can form a network structure via intermolecular interactions. Although the circularly polarized luminescence (CPL) properties of (*R*)-1,1′-binaphthyl-2,2′-dicarboxylic acid with axial chirality could not be measured in either the solution or solid states, those of (*R*)-1,1′-binaphthyl-2,2′-diyl hydrogen phosphate with axial chirality were successfully measured in both states. The solid-state CPL originates from the intramolecular interaction of single molecule, rather than intermolecular interactions in the crystal.

© 2011 Elsevier B.V. All rights reserved.

1. Introduction

The potential application of solid-state fluorescence techniques to organic electroluminescence (EL) devices, optodevice materials, etc., has attracted considerable attention [1]. Although to date, many solid-state organic fluorophores have been reported [2], recently, two-component supramolecular organic fluorophores constructed by weak intermolecular interactions such as a hydrogen bond have attracted much attention. This is because their optical properties can be easily tuned by simply changing the component molecules, without the need for any additional synthesis [3]. However, most of the reported supramolecular organic fluorophores do not have chirality, and there are few reports on chiral two-component supramolecular organic fluorophores that exhibit solid-state chiral optical properties such as solid-state circular dichroism (CD) and circularly polarized luminescence (CPL) [4]. Generally, it is not easy to predict the solid-state optical properties of supramolecular organic complexes comprising new component molecules. Therefore, for a bottom-up approach to designing novel solid-state chiral supramolecular organic fluorophores, it is important to first determine the solid-state chiral optical properties of basic fluorescence supramolecular building blocks that can form

a network structure via intermolecular interactions. In particular, an investigation of the solid-state chiral optical properties of binaphthyl derivatives with axial chirality, one of the most significant basic chiral building blocks, is important. Unfortunately, thus far, the solid-state chiral optical properties of axially chiral binaphthyl derivatives that can form a network structure, for example, a hydrogen-bonded network structure, have not been studied in detail.

In this study, the solid-state chiral optical properties of basic axially chiral binaphthyl derivatives that can form a hydrogen-bonded network structure were investigated. Two chiral binaphthyl acid derivatives were used: (*R*)-1,1′-binaphthyl-2,2′-dicarboxylic acid [(*R*)-**1**] and (*R*)-1,1′-binaphthyl-2,2′-diyl hydrogen phosphate [(*R*)-**2**] (Chart 1).

2. Materials and methods

2.1. General methods

Compound (*R*)-**1** was provided by Mitsubishi Tanabe Pharma Co., Ltd. Compounds (*R*)-**2** and (*S*)-1,1′-binaphthyl-2,2′-diyl hydrogen phosphate [(*S*)-**2**] were purchased from Tokyo Kasei Kogyo Co. Methanol (MeOH) for crystallization, poly(methyl methacrylate) (PMMA) for film-coating, and chloroform (CHCl$_3$) for measurement of the solution-state optical properties were purchased from Wako Pure Chemical Industry. (*R*)-**1**, (*R*)-**2**, and (*S*)-**2** were used after crystallization from MeOH solution.

∗ Corresponding authors. Tel.: +81 06 6730 5880x5241; fax: +81 06 6727 2024.
E-mail addresses: y-matsu@apch.kindai.ac.jp (Y. Matsubara),
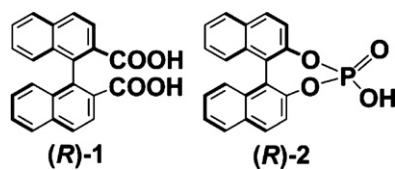y-imai@apch.kindai.ac.jp (Y. Imai).

Chart 1.

2.2. Measurement of solid powder-state and film-state fluorescence spectra

Solid powder-state and film-state fluorescence spectra and absolute photoluminescence quantum yields were measured by the *Absolute PL Quantum Yield Measurement System* (*C9920-02, HAMAMATSU PHOTONICS K. K.*) under an air atmosphere at room temperature. The solid powder-state samples were ground in an agate mortar before measurement. The film-state samples were prepared by using MIKASA SpinCoater Opticoat MS-A100 and PMMA. The excitation wavelength for (*R*)-**2** is 335 nm for the solid powder state and 324 nm for the film state.

2.3. Measurement of solid pellet-state and film-state CD and absorption spectra

The solid pellet-state CD and absorption spectra were measured using a *Jasco J-800KCM spectrophotometer*. The solid pellet-state samples were prepared according to the standard procedure for obtaining glassy KBr matrices [5]. The film-state CD and absorption spectra were measured using a *Jasco J-820 spectrophotometer*. The film-state samples were prepared using PMMA.

2.4. Measurement of solution-state CD and absorption spectra

The solution-state CD and absorption spectra were measured using a *Jasco J-820 spectrophotometer* in CHCl₃ solution (5.0×10^{-5} M) at room temperature.

2.5. Measurement of solid pellet-state and film-state CPL spectra

The solid pellet-state and film-state CPL spectra were measured using a *Jasco CPL-200 spectrophotometer*. The solid pellet-state samples were prepared according to the standard procedure for obtaining glassy KBr matrices [5]. The film-state samples were prepared using PMMA. The excitation wavelengths for the solid pellet-state and film-state **2** were 270 and 300 nm, respectively. The power of the incident beam of the CPL spectrometer was 8.0 μW/0.04 cm² at the installation position of the sample. The CPL spectrum was approached by the simple moving average (SMA).

2.6. Measurement of solution-state CPL spectra

The solution-state CPL spectra were measured using a *Jasco CPL-200 spectrophotometer* in CHCl₃ solution (1.0×10^{-5} M) at room temperature. The excitation wavelength for **2** was 302 nm. The power of the incident beam of the CPL spectrometer was 8.0 μW/0.04 cm² at the installation position of the sample. The CPL spectrum was approached by SMA.

2.7. Theoretical calculation

The geometry of the (*R*)-**2** molecule was optimized by hybrid density functional theory (B3LYP functional) [6]. The excitation energies and rotational strengths of the geometry-optimized molecule were calculated in the time-dependent response function theory using the B3LYP functional [7]. All of these calculations
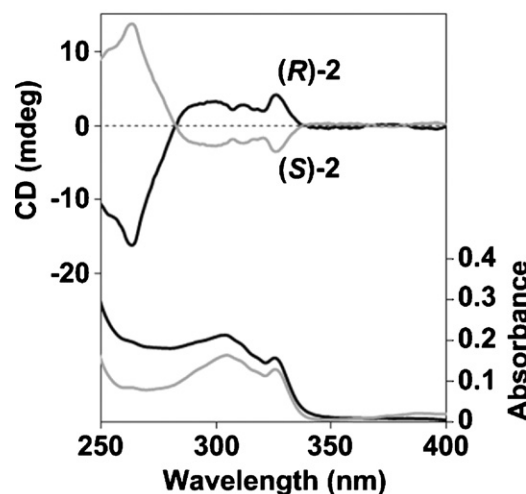

Fig. 1. CD and absorption spectra of (*R*)-**2** (black lines) and (*S*)-**2** (gray lines) in the solid pellet state (KBr pellets).

employed the cc-pVDZ basis set [8]. The Gaussian 03 program was used in these quantum chemical calculations [9].

3. Results and discussion

In order to study the solid-state chiral optical properties of (*R*)-**1** and (*R*)-**2**, we first investigated the solid-state fluorescence properties of these compounds. Unfortunately, the solid powder-state fluorescence of the dicarboxylic acid compound (*R*)-**1** was very weak. On the other hand, the hydrogen phosphate compound (*R*)-**2** exhibited fluorescence in the solid powder state. The solid powder-state fluorescence maximum (λ_{em}) of this compound is 358 nm and the absolute value of the photoluminescence quantum yield (Φ_F) is 0.31.

(*R*)-**1** and (*R*)-**2** are chiral compounds. However, the fluorescence of (*R*)-**1** was able to be hardly observed in the solid powder-state. On the other hand, since (*R*)-**2** had a solid powder-state fluorescence property, it may exhibit CPL in the solid state. Then, in order to study the solid-state CPL of (*R*)-**2**, its solid-state CD spectrum was measured by using a KBr pellet. The solid pellet-state CD and absorption spectra of (*R*)-**2** are shown in Fig. 1 (indicated by black lines).

Peaks originating from the binaphthyl unit were observed in the CD spectrum at ∼339 nm. The circular anisotropy ($g_{CD} = \Delta OD/OD$) factor of the last Cotton effect ($\lambda^{CD} = 325$ nm) is approximately $|7.9 \times 10^{-4}|$. In order to check whether the crystal caused any artifact in the spectrum, the CD and absorption spectra of (*S*)-**2** were measured (Fig. 1, indicated by gray lines). This CD spectrum was found to be a mirror image of the CD spectrum of (*R*)-**2**.

Next, the film-state CD spectrum was measured using a spincoated PMMA film. The film-state CD and absorption spectra of (*R*)-**2** are shown in Fig. 2 (indicated by black lines).

This film-state CD spectrum is similar to the solid-state CD spectrum, and peaks originating from the binaphthyl unit are observed at ∼345 nm. The g_{CD} factor of the last Cotton effect ($\lambda^{CD} = 325$ nm) is approximately $|1.5 \times 10^{-3}|$. Although the film-state CD and absorption spectra of (*S*)-**2** were also measured (Fig. 2, indicated by gray lines), expectedly, this CD spectrum was a mirror image of the CD spectrum of (*R*)-**2**.

Generally, the chemical and physical properties of organic compounds in the solid state are considerably different from those in the solution state. This is so because molecules are densely packed and under the strong influence of neighboring molecules in the solid state. In order to study the origin of these solid-state CD prop-
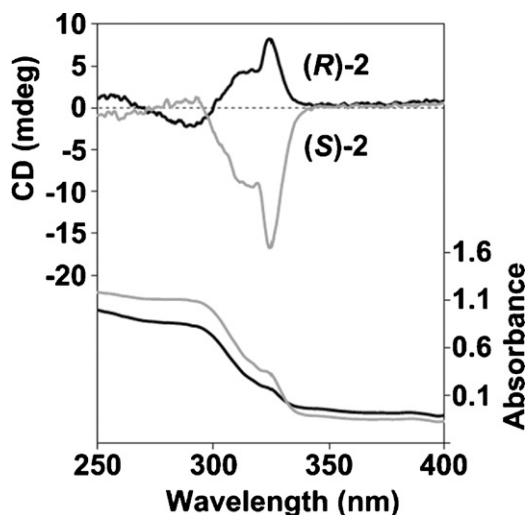
Fig. 2. CD and absorption spectra of (R)-**2** (black lines) and (S)-**2** (gray lines) in the film state (PMMA films).
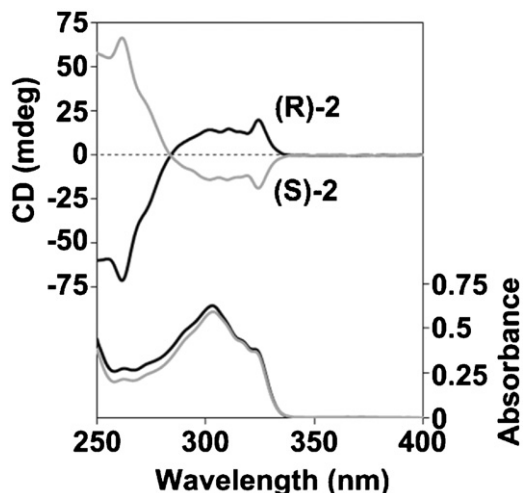

Fig. 3. CD and absorption spectra of (R)-**2** (black lines) and (S)-**2** (gray lines) in the solution state (chloroform solutions).

erties, the solution-state CD spectrum was measured using a CHCl$_3$ solvent. The solution-state CD and absorption spectra of (R)-**2** are shown in Fig. 3 (indicated by black lines).

Interestingly, the solution-state CD spectrum is similar to the solid pellet-state and film-state CD spectra, and peaks originating from the binaphthyl unit were observed in the CD spectrum at ~341 nm. The g_{CD} factor of the last Cotton effect (λ^{CD} = 324 nm)
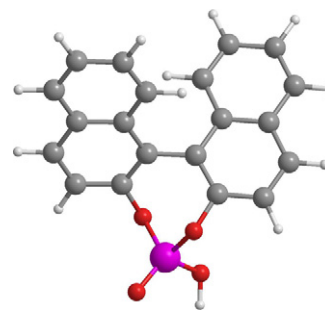

Fig. 5. Theoretically optimized structure of (R)-**2**.

is approximately $|1.6 \times 10^{-3}|$. The solution-state CD spectrum of (S)-**2** (Fig. 3, indicated by gray lines) is also a mirror image of that of (R)-**2**. These results suggest that solid-state CD spectra essentially originate from the intramolecular interactions of single molecules rather than intermolecular interactions between multiple molecules in the crystal. Moreover, they also show that the KBr and PMMA matrices do not affect the CD measurements of this type of compound.

To investigate the origins of the CD intensities of (R)-**2**, the electronic excitations of this molecule were studied theoretically. Fig. 4 shows the theoretically calculated excitation wavelengths (λ) and rotational strengths (R) for a single molecule of (R)-**2**, as well as the CD curves predicted from the calculated data. In Fig. 5, theoretically optimized structure of (R)-**2** is shown.

The calculated data suggest that (R)-**2** should have positive intensity at the longest wavelength edge (~325 nm). Several minor intensities are present at shorter wavelengths, forming − and + peaks centered at ~285 and ~250 nm, respectively. These intensities, together with that at ~325 nm, may form a single positive peak if the peak width broadens. The experimentally observed CD spectra of (R)-**2** in the solid and solution states have positive intensity at the longest wavelength edge. This intensity appears to correspond to the positive intensity at ~325 nm in Fig. 4. This CD intensity mainly originates from the coupling of the HOMO–LUMO π–π^* electronic transitions over each naphthalene ring. The claim that the solid-state CD spectrum of (R)-**2** at around this wavelength originates from electronic interactions within a molecule is supported theoretically. Actually, Fujii and Hirayama have previously reported the crystal structure of (S)-**2** by X-ray crystallographic analysis [10]. Since (S)-**2** has the hydrophobic and hydrophilic regions in the molecule, these regions segregate in the crystal to form hydrophobic and hydrophilic layers. The naphthalene rings aggregate into the hydrophobic layers and their packing pattern is more complex because both of the naphthalene rings that are inclined to each other within a molecule are involved in the packing.

The measurement of a solid-state CPL spectrum of (R)-**2** with a positive Cotton effect was attempted using a KBr pellet and spin-
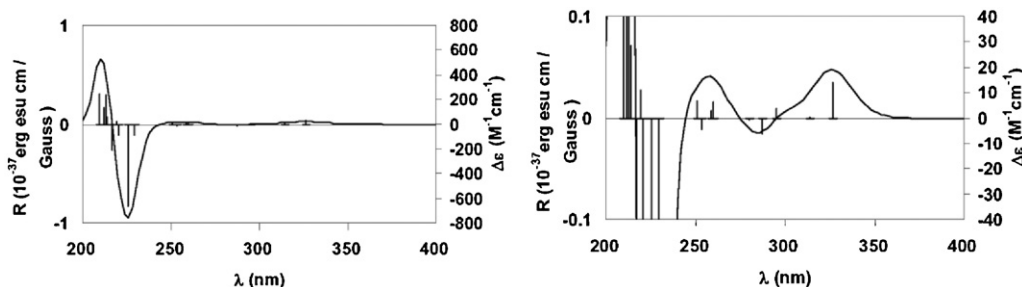

Fig. 4. Calculated excitation wavelengths (λ) and rotational strengths (R) for a single molecule of (R)-**2** (represented by vertical lines, small scale plot [left] and large-scale plot [right]), and the CD curves ($\Delta\varepsilon$) predicted from them. The CD curves were obtained by expanding each vertical line to a Gaussian function with a half-value width of 0.3 eV.
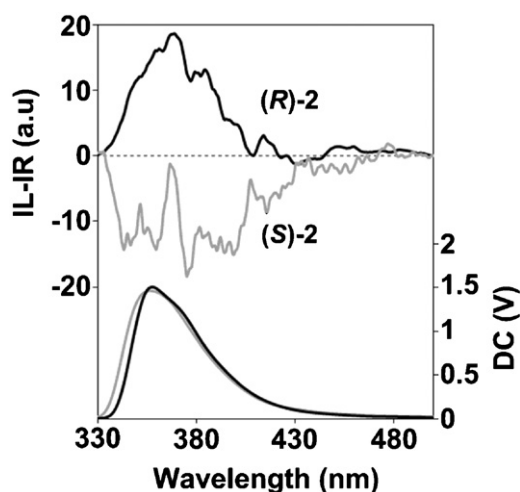
Fig. 6. CPL and fluorescence spectra of (*R*)-**2** (black lines) and (*S*)-**2** (gray lines) in the solid pellet state (KBr pellet).
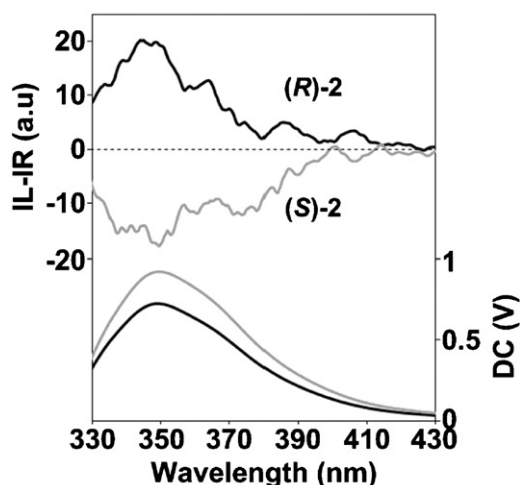

Fig. 7. CPL and fluorescence spectra of (*R*)-**2** (black lines) and (*S*)-**2** (gray lines) in the film state (PMMA film).

coated PMMA film. We successfully obtained the solid-state CPL spectrum of (*R*)-**2**, as shown in Fig. 6 (indicated by black lines) for the solid pellet state and Fig. 7 (indicated by black lines) for the film state.

In both cases, positive CPL spectra were obtained for (*R*)-**2**. Although the solid pellet- and film-state CPL spectra of (*S*)-**2** were also measured (Figs. 6 and 7, indicated by gray lines), expectedly, this CPL spectra were a mirror image of the CPL spectrum of (*R*)-**2**. The circular anisotropy [$g_{em} = 2(I_L - I_R)/(I_L + I_R)$] factor of chiral **2** is approximately $|1.3 \times 10^{-3}|$ for the solid pellet state and $|1.4 \times 10^{-3}|$ for the film state. This shows that the chiral (*R*)-**2** molecule exhibits CPL in the solid state.

In the same way, the measurement of the solution-state CPL spectrum of (*R*)-**2** with a positive Cotton effect was attempted using a CHCl$_3$ solvent in order to study the origin of the solid-state CPL (Fig. 8, indicated by black lines).

Like the CD property, this solution-state CPL spectrum is similar to the solid pellet- and film-state CPL spectra and a positive CPL spectrum was obtained for (*R*)-**2**. In addition, the solution-state CPL spectrum of (*S*)-**2** (Fig. 8, indicated by gray lines) is also a mirror image of that of (*R*)-**2**. The g_{em} factor of chiral **2** is approximately $|1.5 \times 10^{-3}|$. These results suggest that the solid-state CPL of (*R*)-**2** essentially emits from intramolecular interactions
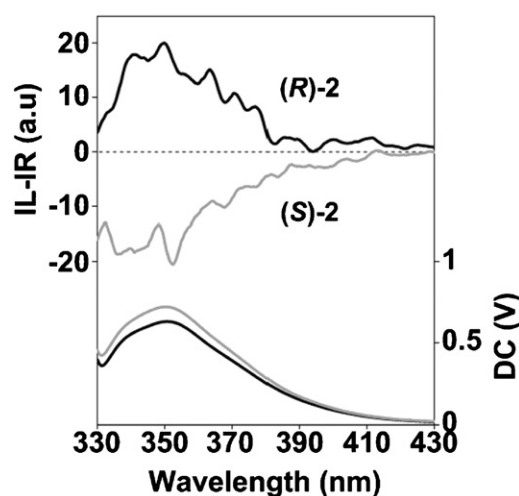

Fig. 8. CPL and fluorescence spectra of (*R*)-**2** (black lines) and (*S*)-**2** (gray lines) in the solution state (chloroform solution).

of a single molecule, rather than from the intermolecular interactions in the crystal, the same as the solid-state CD property of (*R*)-**2**.

4. Conclusion

Although many organic fluorophores lose their fluorescence property in the solid state, (*R*)-1,1′-binaphthyl-2,2′-diyl hydrogen phosphate [(*R*)-**2**] does exhibit this property in the solid state. We successfully observed the CPL spectra of (*R*)-**2** in the solid pellet, film, and solution states. The CD and CPL of (*R*)-**2** originate from the intramolecular interaction of single molecule, rather than intermolecular interactions in the crystal. In addition, it appeared that the KBr and PMMA matrix do not affect the CD and CPL measurements of this type of compound. It is confirmed that this work is useful for the design of novel chiral solid-state supramolecular organic fluorophores composed of axially chiral binaphthyl derivatives.

Acknowledgements

References

[1] (a) J. Shinar, Organic Light-Emitting Devices, Springer, New York/Berlin/Heidelberg, 2004;
(b) K. Müllen, U. Scherf, Organic Light-Emitting Devices, Wiley-VCH, Weinheim, 2006;
(c) C. Jeanne, R. Regis, Dalt. Trans. (2008) 6865–6876;
(d) S. Kappaun, C. Slugovc, J.M. Emil, Phosphorescent organic light-emitting devices: working principle and iridium based emitter materials, Int. J. Mol. Sci. 9 (2008) 1527–1547;
(e) K. Milan, O. Franc, Acetylene-derived strong organic acceptors for planar and nonplanar push–pull chromophores, Accounts Chem. Res. 42 (2009) 235–248;
(f) W.-Y. Wong, C.-L. Ho, Functional metallophosphors for effective charge carrier injection/transport: new robust OLED materials with emerging applications, J. Mater. Chem. 19 (2009) 4457–4482;
(g) K.-L. Chan, P. Sonar, A. Sellinge, Cubic silsesquioxanes for use in solution processable organic light emitting diodes (OLED), J. Mater. Chem. 19 (2009) 9103–9120;
(h) F. Laquai, Y.-S. Park, J.-J. Kim, T. Basche, Excitation energy transfer in organic materials: from fundamentals to optoelectronic devices, Macromol. Rapid Commun. 30 (2009) 1203–1231;

(i) C. Wang, J. Zhang, K. Ryu, A. Badmaev, L.G.D. Arco, C. Zhou, Wafer-scale fabrication of separated carbon nanotube thin-film transistors for display applications, Nano Lett. 9 (2009) 4285–4291;

(j) M.-K. Wei, C.-W. Lin, C.-C. Yang, Y.-W. Kiang, J.-H. Lee, H.-Y. Lin, Emission characteristics of organic light-emitting diodes and organic thin-films with planar and corrugated structures, Int. J. Mol. Sci. 11 (2010) 1527–1545, and references cited therein.

[2] (a) C.W. Tang, S.A. VansSlyke, Organic electroluminescent diodes, Appl. Phys. Lett. 51 (1987) 913–915;

(b) K. Yoshida, Y. Ooyama, S. Tanikawa, Heterocyclic quinol-type fluorophores. Part 2. Solid-state fluorescence enhancement behaviour of benzofurano[3,2-b]naphthoquinol-type clathrate hosts upon inclusion of amine molecules, J. Chem. Soc. Perkin Trans. 2 (2002) 708–714;

(c) K.-C. Wong, Y.-Y. Chien, R.-T. Chen, C.-F. Wang, Y.-T. Liu, H.-H. Chiang, P.-Y. Hsieh, C.-C. Wu, C.H. Chou, Y.O. Su, G.-H. Lee, S.-M. Peng, Ter(9,9-diarylfluorene)s: highly efficient blue emitter with promising electrochemical and thermal stability, J. Am. Chem. Soc. 124 (2002) 11576–11577;

(d) Z. Fei, N. Kocher, C.J. Mohrschladt, H. Ihmels, D. Stalke, Single crystals of the disubstituted anthracene 9,10-(Ph$_2$P=S)$_2$C$_{14}$H$_8$ selectively and reversibly detect toluene by solid-state fluorescence emission, Angew. Chem. Int. Ed. 42 (2003) 783–787;

(e) C.J. Tonzola, M.M. Alam, W.K. Kaminsky, S.A. Jenekhe, New *n*-type organic semiconductors: synthesis, single crystal structures, cyclic voltammetry, photophysics, electron transport, and electroluminescence of a series of diphenylanthrazolines, J. Am. Chem. Soc. 125 (2003) 13548–13558;

(f) J.L. Sott, T. Yamada, K. Tanaka, Novel fluorene based host compounds designed to probe solid-state fluorescence, Bull. Chem. Soc. Jpn. 77 (2004) 1697–1701;

(g) H.-C. Yeh, L.-H. Chan, W.-C. Wu, C.-T. Chen, Non-doped red organic light-emitting diodes, J. Mater. Chem. 14 (2004) 1293–1298;

(h) J.L. Scott, T. Yamada, K. Tanaka, Guest specific solid-state fluorescence rationalised by reference to solid-state structures and specific intermolecular interactions, New J. Chem. 28 (2004) 447–450;

(i) Y. Ooyama, K. Yoshida, Heterocyclic quinol-type fluorophores. Dramatic solid-state fluorescence enhancement behavior of imidazoanthraquinol-type clathrate hosts upon inclusion of various kinds of organic solvent molecules, New J. Chem. 29 (2005) 1204–1212;

(j) D. Berner, C. Klein, M.D. Nazeeruddin, F. de Angelis, M. Castellani, P. Bugnon, R. Scopelliti, L. Zuppiroli, M. Graetzel, Efficient blue light-emitting diodes based on a classical "push–pull" architecture molecule 4,4′-di-(2-(2,5-dimethoxyphenyl)ethenyl)-2,2′-bipyridine, J. Mater. Chem. 16 (2006) 4468–4474;

(k) T.E. Kaiser, H. Wang, V. Stepanenko, F. Wuerthner, Supramolecular construction of fluorescent J-aggregates based on hydrogen-bonded perylene dyes, Angew. Chem. Int. Ed. 46 (2007) 5541–5544;

(l) Y. Ooyama, S. Nagano, M. Okamura, K. Yoshida, Solid-state fluorescence changes of 2-(4-cyanophenyl)-5-[4-(diethylamino)phenyl]-3H-imidazo[4,5-a]naphthalene upon inclusion of organic solvent molecules, Eur. J. Org. Chem. (2008) 5899–5906, and references cited therein.

[3] (a) Y. Mizobe, N. Tohnai, M. Miyata, Y. Hasegawa, A tunable solid-state fluorescence system consisting of organic salts of anthracene-2,6-disulfonic acid with primary amines, Chem. Commun. (2005) 1839–1841;

(b) Y. Mizobe, H. Ito, I. Hisaki, M. Miyata, Y. Hasegawa, N. Tohnai, A novel strategy for fluorescence enhancement in the solid-state: affording rigidity to fluorophores packing, Chem. Commun. (2006) 2126–2128;

(c) S. Oshita, A. Matsumoto, Fluorescence from aromatic compounds isolated in the solid state by double intercalation using layered polymer crystals as the host solid, Langmuir 22 (2006) 1943–1945;

(d) Y. Mizobe, M. Miyata, I. Hisaki, Y. Hasegawa, N. Tohnai, Anomalous anthracene arrangement and rare excimer emission in the solid state: transcription and translation of molecular information, Org. Lett. 8 (2006) 4295–4298;

(e) Y. Mizobe, T. Hinoue, M. Miyata, I. Hisaki, Y. Hasegawa, N. Tohnai, Distinct guest-dependent changes in arrangements of a fluorophore and the corresponding emission modes in a ternary system: transcription and translation of guest molecular information, Bull. Chem. Soc. Jpn. 80 (2007) 1162–1172;

(f) T. Hinoue, Y. Mizobe, I. Hisaki, M. Miyata, N. Tohnai, Modulation of solid-state luminescence quantum efficiency based on CH–O intermolecular interaction, Chem. Lett. 37 (2008) 642–643;

(g) Y. Ooyama, K. Yoshida, Heterocyclic quinol-type fluorophores: solid-state fluorescence change in crystals of benzo[*b*]naphtho[1,2-d]furan-6-one-type fluorophore upon inclusion of organic solvent molecules, Eur. J. Org. Chem. (2008) 2564–2570;

(h) J. Luo, T. Lei, L. Wang, Y. Ma, Y. Cao, J. Wang, J. Pei, Highly fluorescent rigid supramolecular polymeric nanowires constructed through multiple hydrogen bonds, J. Am. Chem. Soc. 131 (2009) 2076–2077;

(i) Y. Imai, K. Murata, K. Kawaguchi, T. Sato, N. Tajima, R. Kuroda, Y. Matsubara, A solid-state fluorescent host system with a 2$_1$-helical column consisting of chiral (1*R*,2*S*)-2-amino-1,2-diphenylethanol and fluorescent 1-pyrenecarboxylic acid, Chem. Asian J. 3 (2008) 625–629;

(j) Y. Imai, K. Nagasaki, K. Murata, K. Kawaguchi, T. Harada, Y. Nakano, T. Sato, M. Fujiki, R. Kuroda, Y. Matsubara, Multiple molecular response columnar host system composed of *rac*-2-amino-1,2-diphenylethanol and 1-fluorenecarboxylic acid, Cryst. Eng. Commun. 10 (2008) 951–953.

[4] (a) Y. Imai, K. Kawaguchi, T. Harada, T. Sato, M. Ishikawa, M. Fujiki, R. Kuroda, Y. Matsubara, Solid-state optical properties of a chiral supramolecular fluorophore consisting of chiral (1*R*,2R)-1,2-diphenylethylenediamine and fluorescent carboxylic acid derivatives, Tetrahedron Lett. 48 (2007) 2927–2930;

(b) Y. Imai, K. Murata, N. Asano, Y. Nakano, K. Kawaguchi, T. Harada, T. Sato, M. Fujiki, R. Kuroda, Y. Matsubara, Selective formation and optical property of a 2$_1$-helical columnar fluorophore composed of achiral 2-anthracenecarboxylic acid and benzylamine, Cryst. Growth Des. 8 (2008) 3376–3379;

(c) Y. Imai, K. Kamon, K. Murata, T. Harada, Y. Nakano, T. Sato, M. Fujiki, R. Kuroda, Y. Matsubara, Preparation of a spontaneous resolution chiral fluorescent system using 2-anthracenecarboxylic acid, Org. Biomol. Chem. 6 (2008) 3471–3475;

(d) Y. Imai, K. Murata, K. Kawaguchi, T. Harada, Y. Nakano, T. Sato, M. Fujiki, R. Kuroda, Y. Matsubara, Complexation behavior of a supramolecular organic fluorophore prepared by solid-state co-grinding crystallization using 2-anthracenecarboxylic acid and (*R*)-1-(2-naphthyl)ethylamine and its optical properties, Eur. J. Org. Chem. (2009) 1335–1339;

(e) Y. Imai, K. Murata, Y. Nakano, T. Harada, T. Sato, N. Tajima, M. Fujiki, R. Kuroda, Y. Matsubara, Solid-state optical properties of a chiral supramolecular organic fluorophore consisting of fluorescent 1-pyrenesulfonic acid and amine molecules, Eur. J. Org. Chem. (2009) 3244–3248;

(f) T. Kinuta, K. Kamon, T. Harada, Y. Nakano, N. Tajima, T. Sato, M. Fujiki, R. Kuroda, Y. Matsubara, Y. Imai, Solid-state chiral supramolecular organic fluorophore having a π-conjugated phenylene ethynylene unit, Eur. J. Org. Chem. (2009) 5760–5764.

[5] R. Kuroda, Y. Saito, Solid-state circular dichroism spectra of tris(diamine)cobalt(III) complexes: decomposition into E and A2 components, Bull. Chem. Soc. Jpn. 49 (1976) 433–436.

[6] A.D. Becke, Density-functional thermochemistry. III. The role of exact exchange, J. Chem. Phys. 98 (1993) 5648–5652.

[7] M.E. Casida, in: D.P. Chong (Ed.), Recent Advances in Density Functional Methods, vol. 1, World Scientific, Singapore, 1995.

[8] (a) T.H. Dunning Jr., Gaussian basis sets for use in correlated molecular calculations. I. The atoms boron through neon and hydrogen, J. Chem. Phys. 90 (1989) 1007–1023;

(b) D.E. Woon, T.H. Dunning Jr., Gaussian basis sets for use in correlated molecular calculations. III. The atoms aluminum through argon, J. Chem. Phys. 98 (1993) 1358–1371.

[9] M.J. Frisch, G.W. Trucks, H.B. Schlegel, G.E. Scuseria, M.A. Robb, J.R. Cheeseman, J.A. Montgomery Jr., T. Vreven, K.N. Kudin, J.C. Burant, J.M. Millam, S.S. Iyengar, J. Tomasi, V. Barone, B. Mennucci, M. Cossi, G. Scalmani, N. Rega, G.A. Petersson, H. Nakatsuji, M. Hada, M. Ehara, K. Toyota, R. Fukuda, J. Hasegawa, M. Ishida, T. Nakajima, Y. Honda, O. Kitao, H. Nakai, M. Klene, X. Li, J.E. Knox, H.P. Hratchian, J.B. Cross, V. Bakken, C. Adamo, J. Jaramillo, R. Gomperts, R.E. Stratmann, O. Yazyev, A.J. Austin, R. Cammi, C. Pomelli, J.W. Ochterski, P.Y. Ayala, K. Morokuma, G.A. Voth, P. Salvador, J.J. Dannenberg, V.G. Zakrzewski, S. Dapprich, A.D. Daniels, M.C. Strain, O. Farkas, D.K. Malick, A.D. Rabuck, K. Raghavachari, J.B. Foresman, J.V. Ortiz, Q. Cui, A.G. Baboul, S. Clifford, J. Cioslowski, B.B. Stefanov, G. Liu, A. Liashenko, P. Piskorz, I. Komaromi, R.L. Martin, D.J. Fox, T. Keith, M.A. Al-Laham, C.Y. Peng, A. Nanayakkara, M. Challacombe, P.M.W. Gill, B. Johnson, W. Chen, M.W. Wong, C. Gonzalez, J.A. Pople, Gaussian 03, Revision C.02, Gaussian, Inc., Wallingford, CT, 2004.

[10] I. Fujii, N. Hirayama, Chiral space formed by (+)-(1*S*)-1,1′-binaphthalene-2,2′-diyl phosphate: recognition of aliphatic L-α-amino acids, Helv. Chim. Acta 85 (2000) 2946–2960.